

Electronic structure of quasicrystals studied by ultrahigh-energy-resolution photoemission spectroscopy

Z. M. Stadnik*

Department of Physics, University of Ottawa, Ottawa, Ontario K1N 6N5, Canada

D. Purdie, M. Garnier, and Y. Baer

Institut de Physique, Université de Neuchâtel, CH-2000 Neuchâtel, Switzerland

A.-P. Tsai

National Research Institute for Metals, Tsukuba Laboratories, 1-2-1 Sengen, Tsukuba-Ibaraki 305, Japan

A. Inoue

Institute for Materials Research, Tohoku University, Sendai 980, Japan

K. Edagawa

Institute of Industrial Science, The University of Tokyo, Roppongi, Minato-ku, Tokyo 106, Japan

S. Takeuchi

Department of Materials Science and Technology, Science University of Tokyo, Noda, Chiba 278, Japan

K. H. J. Buschow

Van Der Waals-Zeeman Laboratorium, Universiteit Amsterdam, 1018 XE Amsterdam, The Netherlands

(Received 13 August 1996)

The results of low-temperature, ultrahigh-resolution ultraviolet photoemission studies of the electronic structure of stable icosahedral $\text{Al}_{65}\text{Cu}_{20}\text{Fe}_{15}$, $\text{Al}_{64}\text{Cu}_{24}\text{Fe}_{12}$, $\text{Al}_{65}\text{Cu}_{20}\text{Ru}_{15}$, $\text{Al}_{65}\text{Cu}_{20}\text{Ru}_{7.5}\text{Fe}_{7.5}$, $\text{Al}_{65}\text{Cu}_{20}\text{Os}_{15}$, $\text{Al}_{70}\text{Pd}_{20}\text{Mn}_{10}$, $\text{Al}_{70}\text{Pd}_{20}\text{Cr}_5\text{Fe}_5$, $\text{Al}_{70.5}\text{Pd}_{21}\text{Re}_{8.5}$, and $\text{Zn}_{60}\text{Mg}_{32}\text{Y}_8$, decagonal $\text{Al}_{65}\text{Co}_{15}\text{C}_{20}$ and $\text{Al}_{70}\text{Co}_{15}\text{Ni}_{15}$, and crystalline $\text{Al}_7\text{Cu}_2\text{Ru}$ and Ni_2MnAl alloys are presented. It is shown that these alloys have a clearly developed Fermi edge, and are thus metallic down to the temperature of measurement (12–45 K). A marked decrease of the spectral intensity toward the Fermi level in quasicrystals is demonstrated to be consistent with the existence of the theoretically predicted pseudogap. With an experimental resolution of 5 meV, no evidence of the theoretically predicted spikiness of the density of states could be observed. A close similarity between the values and unusual dependencies of various physical parameters observed in quasicrystals and in their approximants suggests that they are not the consequence of the long-range quasiperiodicity, but rather result from a complex local atomic order. A review of the electronic properties of quasicrystals is also presented. [S0163-1829(97)07815-6]

I. INTRODUCTION

Quasicrystals (QC's), which were discovered in 1984,¹ are an interesting form of the solid state which differs from the other two known forms, crystalline and amorphous, by possessing a new type of long-range translational order, *quasi-periodicity*, and a noncrystallographic orientational order associated with the classically forbidden symmetry axes.^{2–5} The majority of known QC's are either icosahedral (*i*) or decagonal (*d*) alloys. A few known octagonal^{3,6} and dodecagonal^{3,7} alloys cannot be produced in sufficient quantities to allow studies of their physical properties. A central problem in condensed-matter physics is to determine whether quasiperiodicity leads to physical properties which are significantly different from those of crystalline and amorphous materials.

The first few years of studies of QC's revealed that their physical properties are disappointingly similar to those of the corresponding crystalline or the amorphous counterparts.^{3,4,8}

It was only realized later that the first QC's, which were thermodynamically *metastable*, possessed significant structural disorder, as manifested in the broadening of x-ray- and/or electron-diffraction lines. In addition, they contained non-negligible amounts of second phases. These poor quality samples impeded the detection of those properties which could be intrinsic to quasiperiodicity.

A significant development in the studies of both structural and physical properties of QC's occurred at the end of the 1980s, when thermodynamically *stable* QC's were discovered.^{3–5,8} These QC's possess a high degree of structural perfection comparable to that found in the best periodic alloys, as evidenced by resolution-limited width of the Bragg peaks⁹ and/or the observation of dynamical diffraction.¹⁰ Several unusual physical properties have been found in the most intensively studied *i* alloys.^{2–5,8} First, their most salient feature, which is completely unexpected for alloys consisting of normal metallic elements, is the very high value of the electrical resistivity ρ (or the very low value of the electrical

conductivity σ). For example, the low-temperature $\rho(\sigma)$ values can reach about $10\,000\ \mu\Omega\ \text{cm}$ ($100\ \Omega^{-1}\ \text{cm}^{-1}$) in the Al-Cu-Fe *i* alloys,^{11–16} about $25\,000\ \mu\Omega\ \text{cm}$ ($40\ \Omega^{-1}\ \text{cm}^{-1}$) in the Al-Pd-Mn *i* alloys,^{17–20} about $60\,000\ \mu\Omega\ \text{cm}$ ($17\ \Omega^{-1}\ \text{cm}^{-1}$) in the Al-Cu-Ru *i* alloys,^{21–23} about $100\,000\ \mu\Omega\ \text{cm}$ ($10\ \Omega^{-1}\ \text{cm}^{-1}$) in the Al-Cu-Os *i* alloys,²⁴ and extraordinary high (low) values of the order of $10^7\ \mu\Omega\ \text{cm}$ ($0.1\ \Omega^{-1}\ \text{cm}^{-1}$) in the Al-Pd-Re *i* alloys.^{20,25–29} These $\rho(\sigma)$ values are several orders of magnitude larger (smaller) than those of the constituent metals and of the amorphous alloys, and are comparable to those of doped semiconductors. The above experimental σ values are smaller than the Mott's "minimum metallic conductivity" of $200\ \Omega^{-1}\ \text{cm}^{-1}$ for the metal-insulator transition.³⁰ It was even suggested that the Al-Pd-Re *i* alloys are insulators at low temperatures.^{26,27} Second, the temperature coefficient of $\rho(\sigma)$ of these *i* alloys is generally negative (positive),^{2–4,8,12,13,15–29} which is inconsistent with the expected behavior for metals. Third, the $\rho(\sigma)$ values are extremely sensitive to the sample composition,^{15,20,21,25,26,28} which is reminiscent of doping effects in semiconductors. Even for the same nominal composition, they can change by more than an order of magnitude for samples produced from the same batch.^{25,29} This means the composition inhomogeneities of a fraction of an at. % can significantly influence the electronic properties of the *i* alloys. Fourth, the resistivity of these *i* alloys increases as their structural quality improves (by annealing which removes the defects),^{8,20,25,27} in contrast to the behavior of typical metals. Other unexpected anomalies in the transport properties of *i* alloys involve^{2–4,8} a very low electronic contribution to the specific heat γ ,^{15,21,26,27} large and strongly temperature-dependent Hall coefficient and thermoelectric power,^{14,21,27,31} the unusual linear frequency dependence of the optical conductivity and an absence of the usual Drude contribution characteristic of metals,^{32,33} or the very small values of the thermal conductivity.^{34,35} From a magnetic point of view, stable *i* alloys of high structural quality are unusual in that they are diamagnetic^{19,36} in spite of containing significant concentrations of transition-metal (TM) atoms.

QC's of decagonal symmetry exhibit anisotropic physical properties: the electrical resistivity has metallic characteristics along the periodic direction, and shows a nonmetallic behavior in the quasiperiodic plane.³⁷ Anisotropies in the Hall effect, thermopower, and thermal and optical conductivities were also observed.^{37–39} The *d* alloys Al-Co-Cu and Al-Co-Ni were also shown to be diamagnetic over a wide temperature range.⁴⁰

A fundamental question in the physics of QC's is the origin of the unusually low values of the electrical conductivity. The interpretation suggested first, which is still prevailing, is based upon a Hume-Rothery mechanism,⁴¹ which implies the existence of a pseudogap in the electronic density of states (DOS) in the vicinity of the Fermi level E_F .⁴² Initially, the Hume-Rothery mechanism was invoked, both from experimental⁴³ and theoretical analyses,⁴⁴ in relation to the problem of stability of QC's. It was later linked⁴⁵ to the observed small- σ values through the Einstein equation³⁰ $\sigma = e^2 D N(E_F)$, in which D is the electron diffusion coefficient (diffusivity) and $N(E_F)$ designates $\text{DOS}(E_F)$. The correlation between the low σ and the low $N(E_F)$ was based

upon the experimental observation of the very small value of γ ,^{8,15,21,26,27,45} which is directly proportional to $N(E_F)$. The support for the Hume-Rothery mechanism in *i* alloys also comes from the results of the NMR (Ref. 46) and optical conductivity experiments.^{33,47} However, the optical conductivity data³⁹ for *d* alloys could not be reconciled with the existence of a pseudogap in the $\text{DOS}(E_F)$. The reduced $N(E_F)$ is also consistent with the observed diamagnetism.^{19,36,40} Furthermore, almost all low-energy-resolution soft-x-ray emission (SXE), soft-x-ray absorption (SXA), photoemission spectroscopy (PES), x-ray photoelectron spectroscopy (XPS), and inverse photoemission spectroscopy (IPES) experiments which, as opposed to the experimental techniques mentioned earlier, probe DOS directly at energies in the vicinity of E_F , have been interpreted^{48–50} in terms of the presence of the pseudogap in the DOS around E_F in *i* alloys. However, low-energy-resolution PES experiments on *d* alloys could not find evidence of the existence of such a pseudogap.^{51,52} The notion of a structure-induced pseudogap in the DOS around E_F results not only from a theoretical analysis based on the nearly-free-electron approximation^{44,53} but is also supported by the electronic structure calculations for the lowest-order crystalline approximants of *i* alloys,^{54–59} including the approximants containing the TM atoms.^{54,56,58,59} However, the electronic structure calculations for *d* alloys are contradictory: while the calculations based on a model approximant $\text{Al}_{66}\text{Co}_{14}\text{Cu}_{30}$ predict⁶⁰ the existence of a well-pronounced and wide pseudogap in the DOS around E_F , those based on several variants of the Burkov model⁶¹ predict that no pseudogap exists for the most stable *d* structures.⁶²

Apart from its seeming simplicity expressed in the relation $Q = 2k_F$ (Q is the magnitude of the reciprocal-lattice vector, and k_F is the radius of the Fermi sphere), which corresponds to the Fermi sphere touching a Brillouin-zone plane, the Hume-Rothery mechanism is particularly appealing because it can explain qualitatively why stable QC's have both the lowest values of σ and γ . It can also be used to rationalize qualitatively why stable QC's exist only in a rather narrow composition range (a small composition change can shift the E_F away from the DOS minimum). It was argued that the pseudogap enhancement of the cohesive energy is more efficient in QC's than in the crystalline approximants because the pseudo-Brillouin-zone is nearly spherical in the latter^{33,44,54,55} due to the high multiplicity of the Bragg planes resulting from the high symmetry of the icosahedral point group.

On the experimental side, one observes the dramatic changes of σ (up to two orders of magnitude) with composition^{15,20,21,25,26,28} and structural quality^{16,27,63} for *i* samples whose values of γ differ only by up to about 10%. For example, the values of σ (at 2 K) and γ for *i*-Al₆₉Pd₁₉Re₁₂ are respectively $1000\ \Omega^{-1}\ \text{cm}^{-1}$ and $0.28\ \text{mJ/mol K}^2$ (Ref. 28). The corresponding values for *i*-Al₆₇Pd₂₃Re₁₀ are $100\ \Omega^{-1}\ \text{cm}^{-1}$ and $0.25\ \text{mJ/mol K}^2$ (Ref. 28). This is at variance with the expected proportionality between σ and γ , and indicates that the small values of σ in *i* alloys cannot be associated only with the Hume-Rothery-type mechanism. This mechanism also cannot explain the increase of σ with temperature and with the removal of defects (in fact, it predicts just the opposite

behavior). The majority of stable *i* alloys contain TM atoms whose *3d* states dominate the $N(E_F)$.⁴⁹ Since σ in the Einstein equation is proportional to the product $DN(E_F)$, the unusually small values of σ may originate from the unusually small values of the electron diffusivity. The arguments presented above indicate that the possible pseudogap in the $DOS(E_F)$ may not be the main reason for the very small σ values observed in QC's and for their unusual transport properties.

The temperature and defect dependencies of σ , as well as the temperature dependencies of other transport parameters, are even more difficult to understand. Within the semiquantitative band-structure model, which is based on the calculated electronic structure for a given approximant and on the Boltzmann theory on the two-dimensional Penrose lattice,^{56,58,60} the observed temperature dependence of σ is argued to be explained by considering the interband transitions resulting from electron-phonon and electron-electron inelastic scattering, whereas the dependence of σ on the structural quality is suggested to result from interband transitions due to elastic scattering by the random phason strain. Essential to this model is the predicted very fine sharp-peaked structure of the DOS. This predicted DOS spikiness is associated with a large number of nondegenerate flatbands in QC's, and is believed to be amplified by the presence of TM atoms.^{56,58,60} Two energy scales are thus involved in the band-structure approach: one associated with the width of a pseudogap (about 500–1000 meV), and the other related to the width of the spiky peaks (about 10–20 meV). Within the spirit of the band-structure approach, a recent model based on phonon and impurity scattering in real, “dirty” QC's has been proposed.⁶⁴ It introduced a fractional multicomponent Fermi surface consisting of many electron and hole valleys which lead to the intravalley and intervalley scattering processes. These processes are claimed to provide a natural explanation for a number of unusual transport properties of QC's.⁶⁴

In the last few years, some more exotic mechanisms, which invoke the concepts of tunneling, localization, critical states, and fractons, were proposed to explain the unusual transport properties of QC's. The first such mechanism, which is completely qualitative in nature and which claims to explain many of the physical properties of QC's, is based upon an internal structural model.^{65,66} It advocates that an *i* alloy consists of two building units: a conductive *i* block enveloped by an insulating layered-structure network. The electrical conduction would occur via tunneling through the insulating network, which should lead to deviations from Ohm's law. However, the law was shown⁶⁷ to be obeyed perfectly in the *i*-Al-Cu-Fe film for bias voltages varying by seven orders of magnitude. Another unconventional qualitative model^{16,68} to explain the unusual transport properties of QC's is based upon the idea of electron localization, which was first suggested by Kimura *et al.* (Ref. 69). The model^{16,68} assumes that the conduction occurs by hopping between states which tend to be localized around some structural units (clusters) separated by about a few nm. Within a band-structure picture, this hopping mechanism corresponds to the interband transitions. A model which is similar in spirit is a recent hierarchically variable-range hopping model⁷⁰ in which QC's are presented as a hierarchy of

clusters.^{70,71} The model claims to explain qualitatively some of the unusual transport properties of QC's. A recent model⁷² based on an electron-fracton scattering explains qualitatively some of the transport and acoustic dependencies observed in QC's. It even predicts the possibility of superconductivity resulting from a fracton-mediated electron pairing.

It is clear from the above review that no well-established theory which would account for the observed unusual properties of QC's is available at present. However, there are a few features common to some of the theoretical models mentioned above. One of them is the predicted pseudogap in the $DOS(E_F)$, which is believed to be responsible, at least partially, for the stability of QC's and for the observed low values of σ . The other feature is the predicted presence of a spiky structure of the DOS. Although the pseudogap seems to be a *generic* property of QC's, it is not a *specific* property distinguishing the quasiperiodic from the periodic or aperiodic phases because such a pseudogap is also believed to be present in some amorphous⁷³ and crystalline^{74,75} alloys. This is consistent with the fact that a pseudogap is due to a short-range order. A property specific to a quasicrystalline order seems to be the predicted DOS spikiness, which does not occur in crystalline or amorphous systems.

As mentioned earlier, the main support for the concept of a pseudogap in the DOS around E_F comes from the experiments which probe the $DOS(E_F)$ indirectly. Although all low energy-resolution (0.2–0.7 eV) SXE and SXA experiments conducted on both stable and metastable QC's were interpreted as a definite spectroscopic evidence of the presence of a pseudogap,⁴⁸ such an interpretation is open to criticism. This interpretation is based upon three apparent observations: a shift (of about a few tenth of eV) of the edge of the Al *3p* valence-state spectrum toward higher binding energies, a reduction of the Al *3p* intensity at E_F , and a “bending” of the Al *p* conduction-state spectrum as compared to the corresponding features of the Al metal and of crystalline alloys.⁴⁸ The first observation is not convincing in view of the large uncertainty in determining the position of E_F , which must be determined from separate XPS measurements (as will be demonstrated in Sec. III, the claimed uncertainty of 0.1–0.2 eV for the Al *p* spectra seems to be underestimated). The other two observations rely on the intensity scale and its rather arbitrary normalization for different spectra. Even more surprising is the claim⁷⁶ of the experimental evidence based on the SXA technique for the presence of the DOS spikes in the conduction Al *p* band. This claim is based on the apparent observation of the low intensity of the Al *p* band as compared to that of other Al-based alloys and of the Al metal. This low intensity is not related to the DOS spikiness because the SXA technique cannot detect any spiky features in the DOS due to the severe lifetime broadening effects inherent to this technique.⁴⁹

PES measurements with ultrahigh energy resolution are essential^{49,52} in order to verify the hypothesis of the DOS spikiness in QC's unambiguously. So far, no direct evidence of the presence of this spikiness has been found as most of the previously published PES investigations were limited to resolutions larger than 230 meV (Refs. 49, 52, and 77). Based on the claim of the absence of a sharp Fermi edge, two PES studies concluded that there is a pseudogap in the $DOS(E_F)$ in *i*-Al-Cu-Fe (Ref. 77) and in *i*-Al-Pd-Mn.⁷⁸

However, the conclusion common to these two previous studies must be questioned, given that they were both carried out at room temperature.^{77,78} In addition, the data of Wu *et al.* (Fig. 3 in Ref. 78) do not continue sufficiently far beyond the Fermi level into the positive-energy region to allow the background contribution to the spectrum to be estimated. The background contribution can severely alter the shape of the photoemission spectrum. Consequently, the unusual form of the DOS close to E_F observed in Ref. 78 is not incompatible with a simple Fermi edge. In order to establish the presence or absence of a Fermi edge reliably, measurements must be performed at low temperatures, where thermal broadening of the Fermi-Dirac function is small, and with an instrumental contribution of the same order of magnitude as $k_B T$.⁷⁹ In this paper we report the results of an extensive study of the electronic structure of most known stable QC's, where it is demonstrated that only through use of these stringent conditions can firm conclusions regarding the detailed form of the near- E_F DOS be drawn.

II. EXPERIMENT

Thermodynamically stable QC's of nominal compositions i -Al₆₅Cu₂₀Fe₁₅, i -Al₆₄Cu₂₄Fe₁₂, i -Al₆₅Cu₂₀Ru₁₅, i -Al₆₅Cu₂₀Ru_{7.5}Fe_{7.5}, i -Al₆₅Cu₂₀Os₁₅, i -Al₇₀Pd₂₀Mn₁₀, i -Al₇₀Pd₂₀Cr₅Fe₅, i -Al_{70.5}Pd₂₁Re_{8.5}, i -Zn₆₀Mg₃₂Y₈, d -Al₆₅Co₁₅Cu₂₀, and d -Al₇₀Co₁₅Ni₁₅ were prepared as described elsewhere.^{24,25,80-85} All samples were characterized by x-ray diffraction and electron microscopy, both techniques showing the samples to be single phase. Bragg-peak widths were resolution limited. To characterize the alloys studied further, electrical conductivity and magnetic-susceptibility measurements were carried out respectively for Al-Cu-Fe, Al-Cu-Ru, Al-Pd-Re, and Al-Cu-Ru i alloys. The results are in agreement with published data.^{11-16,19-23,25-29,36} For comparison purposes, a tetragonal Al₇Cu₂Ru (Ref. 86) and a Heusler alloy Ni₂MnAl of the L2₁ structure were also used.

The samples were mounted on the cold finger of a liquid-He cryostat and, while held at the lowest measurement temperature, were cleaned *in situ* ($\sim 10^{-10}$ Torr) by repeated scraping with a diamond file until no surface contamination could be detected.⁸⁷ The low temperature prevents any structural reorganization of the sample upon scraping, and it therefore seems reasonable to assume that this process results in samples which maintain quasicrystallinity at the surface. Moreover, given the statistical distribution of surfaces produced, the photoemission data correspond, as closely as possible, to a realistic estimate of the DOS of the measured alloys. Valence-band spectra obtained from different regions of a given sample, as well as from several samples corresponding to a given composition, were reproducible. We therefore believe that the spectra represent the intrinsic features of the QC's studied. The ultraviolet photoelectron spectroscopy (UPS) spectrometer was equipped with a high-intensity He discharge lamp (Gammadata) producing a He I line at 21.2 eV and a He II line at 40.8 eV, and a high-resolution Scienta SES200 hemispherical analyzer. The instrumental resolution was determined by fitting the Fermi edge of Ag, evaporated *in situ* onto the previously measured samples, with the convolution of a Gaussian and the product

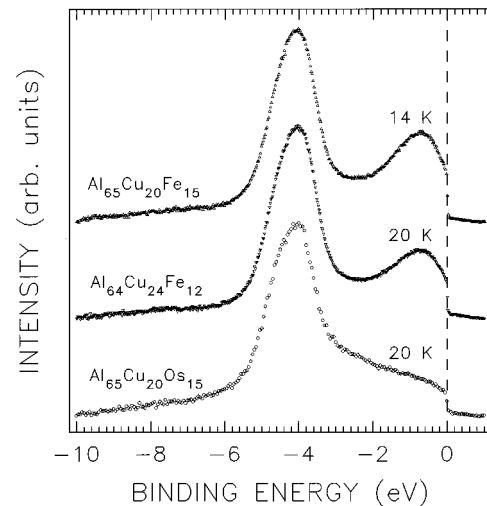


FIG. 1. Low-temperature He II valence bands of Al-Cu-TM (TM = Fe, Os) i alloys. The energy resolution is ~ 30 meV. The spectra have been normalized to give a constant height between the maximum and minimum count.

of a linear DOS and the Fermi-Dirac function at the appropriate temperature.⁷⁹ The full width at half-maximum (FWHM) of the Gaussian is the only adjustable parameter in this procedure and gives directly the instrumental resolution. For high-resolution spectra this was determined to be ≤ 10 meV. The uncertainty in the determination of E_F is less than 0.5 meV. The UPS valence bands presented here are corrected for the secondary-electron background.⁵²

III. RESULTS AND DISCUSSION

A. Structure of valence bands

1. Icosahedral alloys

The low-temperature He II valence bands of i alloys of the Al-Cu-TM series (Figs. 1 and 2) have a similar two-peak

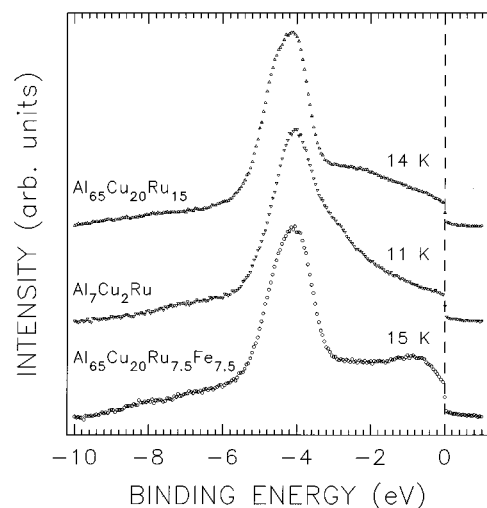


FIG. 2. Low-temperature He II valence bands of Al-Cu-(Ru,Fe) i alloys and crystalline Al₇Cu₂Ru. The energy resolution is ~ 30 meV. The spectra have been normalized to give a constant height between the maximum and minimum count.

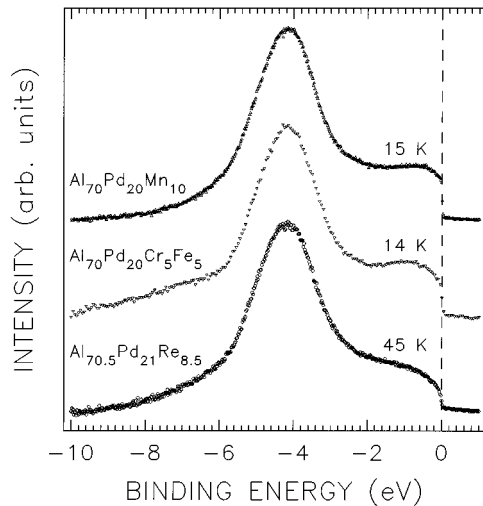


FIG. 3. Low-temperature He II valence bands of Al-Pd-TM *i* alloys. The energy resolution is ~ 30 meV. The spectra have been normalized to give a constant height between the maximum and minimum counts.

structure. The feature at a binding energy (E_B) of about -4.1 eV is mainly due to the Cu $3d$ -derived states, whereas the feature close to E_F is predominantly due to states of Fe $3d$, Os $5d$, or Ru $4d$ character, as appropriate. This assignment is based on previous resonance PES studies of the *i* alloys of this series.^{49,87} The contribution of the Al *sp*-like states is not observed in the presented valence bands due to significantly smaller photoionization cross sections for Al *sp* orbitals as compared to those for TM *d* orbitals for the He II and He I photon energies used here.⁸⁸ The intensity difference between the Fe $3d$ features of the *i* alloys Al₆₄Cu₂₄Fe₁₂ and Al₆₅Cu₂₀Fe₁₅ (Fig. 1) is consistent with the compositions of these alloys, confirming the validity of the surface preparation procedure. A close similarity between the valence bands of *i*-Al₆₅Cu₂₀Ru₁₅ and crystalline Al₇Cu₂Ru (Fig. 2) can be noticed.

The low-temperature He II valence bands of *i* alloys of the Al-Pd-TM series (Fig. 3) also have a two-peak structure. The feature at $E_B \approx -4.2$ eV is mainly due to the Pd $4d$ -like states, and the feature close to E_F is predominantly due to states of Mn, Fe, Cr $3d$ and Re $5d$ character, as appropriate.^{89–92}

The He II valence band of *i*-Zn₆₀Mg₃₂Y₈ at 14 K (Fig. 4) has the most prominent feature due to Zn $3d$ -like states. The use of high energy resolution enables a clear detection of the Zn $3d_{5/2}$ and $3d_{3/2}$ components located at E_B 's of $-9.942(3)$ and $-9.457(1)$ eV. These E_B 's should be compared with the values of $-9.77(10)$ and $-9.23(10)$ eV in pure Zn at room temperature.⁹³ The states of the Zn $3d$ character are thus shifted away from E_F as compared to the states in Zn metal. The Zn $3d_{5/2}$ - $3d_{3/2}$ splitting of $0.485(4)$ eV is smaller than the corresponding splitting of $0.54(2)$ eV in Zn metal.⁹³ The weak satellite He II* line at 48.4 eV produced in the He lamp⁹⁴ is responsible for the “ghost” Zn $3d$ feature at $E_B \approx -2$ eV (Fig. 4).

There are two salient features of the valence bands in Figs. 1–4. First, the presence of a Fermi edge is indicated in

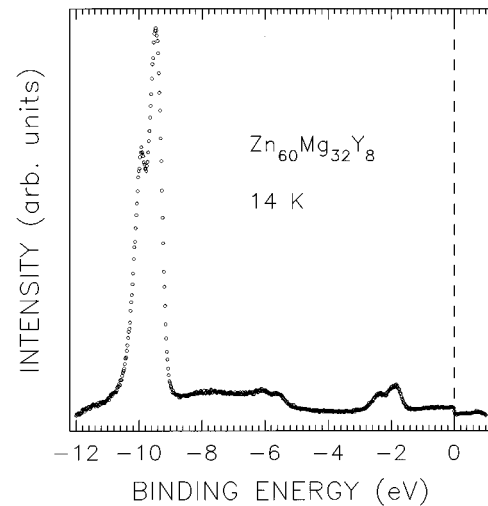


FIG. 4. Low-temperature He II valence band of *i*-Zn₆₀Mg₃₂Y₈ measured with an energy resolution of 28 meV.

all the *i* alloys studied. Second, as compared to that of Al-Cu-TM and Al-Pd-TM alloys, a significantly lower spectral intensity at E_F is observed in the *i*-Al_{70.5}Pd₂₁Re_{8.5} alloy.

2. Decagonal alloys

The low-temperature He II valence bands of two *d* alloys (Fig. 5) have a similar structure to that observed previously.^{51,52} As shown earlier with the resonance PES technique,⁵² the feature close to E_F is predominantly due to states of Co $3d$ character in *d*-Al₆₅Co₁₅Cu₂₀, and of Co and Ni $3d$ character in *d*-Al₇₀Co₁₅Ni₁₅. The feature at $E_B \approx -4.2$ eV in the valence band of *d*-Al₆₅Co₁₅Cu₂₀ is principally due to the Cu $3d$ -derived states.⁵² The feature close to E_F in the metallic Ni₂MnAl is principally due to states of Ni and Mn $3d$ character. The two clear characteristics of the spectra in Fig. 5 are the presence of a Fermi edge

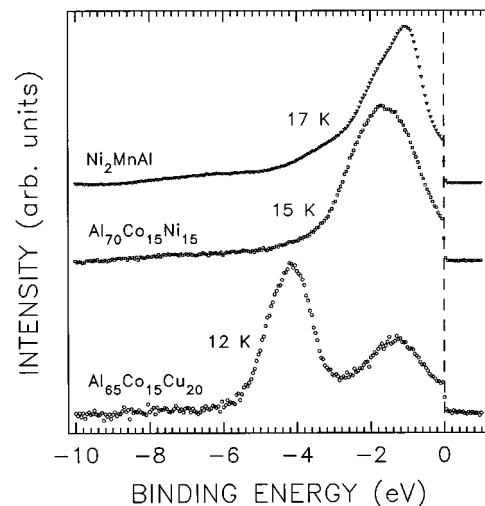


FIG. 5. Low-temperature He II valence bands of two *d* alloys Al₆₅Co₁₅Cu₂₀ and Al₇₀Co₁₅Ni₁₅ and of a Heusler alloy Ni₂MnAl. The energy resolution is ~ 30 meV. The spectra have been normalized to give a constant height between the maximum and minimum count.

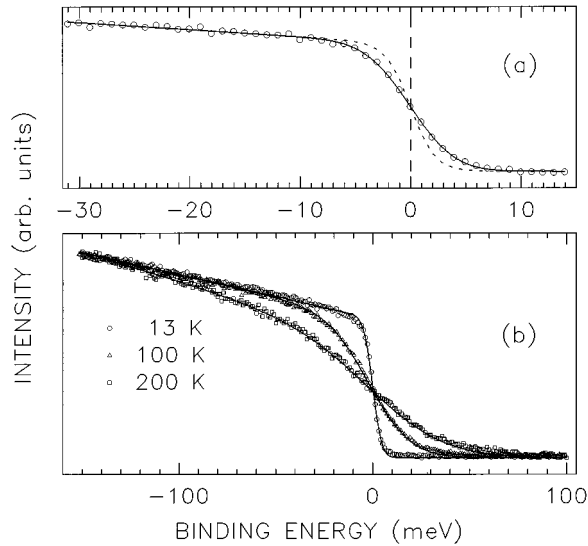


FIG. 6. (a) Near- E_F He I valence band of $i\text{-Al}_{65}\text{Cu}_{20}\text{Fe}_{15}$ at 13 K. The solid line is a fit to a linearly decreasing intensity multiplied by the Fermi-Dirac function at 13 K (broken curve) and convoluted with a Gaussian whose FWHM is equal to 6.2(2) meV. Note that the step between the data points is 1 meV. (b) Near- E_F He I valence bands of $i\text{-Al}_{65}\text{Cu}_{20}\text{Fe}_{15}$ measured at different temperatures. The solid lines are the fits as described in (a). Note the different E_B scales in (a) and (b).

in the d alloys studied, and, as compared to that in the crystalline Ni_2MnAl , the shift of the features due to the TM 3d states away from E_F .

B. Valence bands in the vicinity of E_F

To investigate the electronic structure of QC's very close to E_F , the near- E_F valence-band region was examined with the highest-energy resolution presently available to us.

1. Icosahedral alloys

A high-energy-resolution spectrum for the $i\text{-Al}_{65}\text{Cu}_{20}\text{Fe}_{15}$ alloy is shown in Fig. 6(a). A clearly developed Fermi edge, which can be perfectly fitted using a Fermi-Dirac function convoluted with a Gaussian function representing the instrumental broadening [Fig. 6(a)], is observed. The temperature evolution of the Fermi edge of $i\text{-Al}_{65}\text{Cu}_{20}\text{Fe}_{15}$ follows exactly that of a Fermi-Dirac function [Fig. 6(b)]. Similar near- E_F spectra were also found for $i\text{-Al}_{65}\text{Cu}_{20}\text{Ru}_{7.5}\text{Fe}_{7.5}$ (Fig. 7) and $i\text{-Al}_{70}\text{Pd}_{20}\text{Mn}_{10}$.⁹⁵ Figure 8 presents the near- E_F spectra of $i\text{-Al}_{65}\text{Cu}_{20}\text{Os}_{15}$ and $i\text{-Zn}_{60}\text{Mg}_{32}\text{Y}_8$ and of Ag evaporated onto them. Again, a perfectly developed Fermi edge is observed.

The behavior of the $i\text{-Al}_{70.5}\text{Pd}_{21}\text{Re}_{8.5}$ alloy was found to be different from the other QC's studied in that we were unable to cool it down as far as all the other samples. This may be related to the fact that the low-temperature thermal conductivity of the $i\text{-Al-Pd-Re}$ alloys³⁵ is the lowest among known QC's (it is about an order of magnitude lower³⁵ than in $i\text{-Al-Pd-Mn}$ alloys³⁴). The lowest temperature achieved was 45 K.⁹⁶ However, all samples of this alloy displayed a clear Fermi edge. This can be seen by comparing a near- E_F spectrum of $i\text{-Al}_{70.5}\text{Pd}_{21}\text{Re}_{8.5}$ with that of Ag evaporated

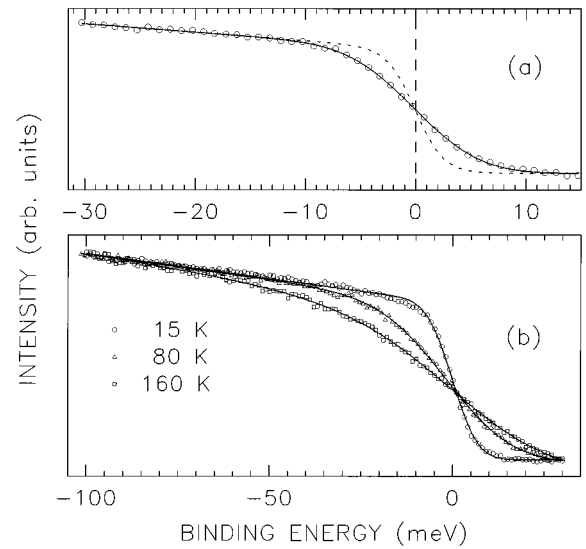


FIG. 7. (a) Near- E_F He I valence band of $i\text{-Al}_{65}\text{Cu}_{20}\text{Ru}_{7.5}\text{Fe}_{7.5}$ at 15 K. The solid line is a fit to a linearly decreasing intensity multiplied by the Fermi-Dirac function at 15 K (broken curve) and convoluted with a Gaussian whose FWHM is equal to 9.8(2) meV. Note that the step between the data points is 1 meV. (b) Near- E_F He I valence bands of $i\text{-Al}_{65}\text{Cu}_{20}\text{Ru}_{7.5}\text{Fe}_{7.5}$ measured at different temperatures. The solid lines are the fits as described in (a). Note the different E_B scales in (a) and (b).

onto the alloy (Fig. 9). The temperature dependence of the near- E_F spectra of this alloy was found to follow that of the Fermi-Dirac function.

The presence of a clearly developed Fermi edge (Figs. 6–9 and Ref. 95) and its expected evolution with temperature (Figs. 6 and 7 and Ref. 95) in high-quality, stable i

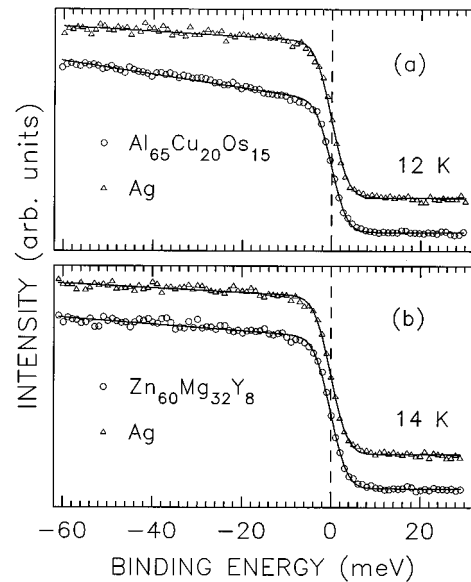


FIG. 8. Near- E_F low-temperature He I valence bands of (a) $i\text{-Al}_{65}\text{Cu}_{20}\text{Os}_{15}$ and Ag evaporated onto it and (b) $i\text{-Zn}_{60}\text{Mg}_{32}\text{Y}_8$ and Ag evaporated onto it. The solid curves are the fits to a linearly decreasing intensity multiplied by the Fermi-Dirac function at an appropriate temperature and convoluted with a Gaussian whose FWHM is 5.4(2) in (a) and 5.2(2) meV in (b).

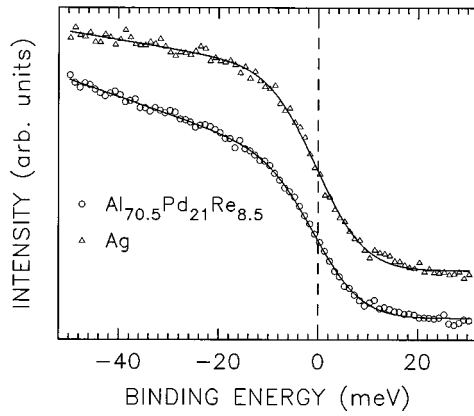


FIG. 9. Near- E_F He I valence bands of i -Al_{70.5}Pd₂₁Re_{8.5} and Ag evaporated onto it measured at 45 K with an experimental resolution of 6 meV. The solid curves are the fits to a linearly decreasing intensity multiplied by the Fermi-Dirac function at 45 K (the convolution with the instrumental broadening function produces a negligible effect at this temperature).

alloys constitute a direct and convincing proof that these alloys, in spite of their unusually high values of ρ , are metallic down to the temperature of measurement (12–45 K). In a recent study of i -Al₆₅Cu₂₀Ru₁₅ with electron-energy-loss spectroscopy (an energy resolution of 120 meV) a sharp Fermi edge was also observed.⁹⁷ Labeling such i alloys “marginally metallic” (Al-Cu-Fe and Al-Pd-Mn, Ref. 98), “semiconducting” (Al-Cu-Ru, Ref. 31), or “insulating” (Al-Pd-Re, Refs. 26, 27, and 98) is not, therefore, justified.

2. Decagonal alloys

The high-energy-resolution near- E_F spectra of d -Al₆₅Co₁₅Cu₂₀ and d -Al₇₀Co₁₅Ni₁₅, and of Ag evaporated onto them, are shown in Fig. 10. A clearly developed Fermi edge, which can be fitted using a Fermi-Dirac function convoluted with a Gaussian function representing the instrumental broadening, can be seen (Fig. 10). As shown in Fig. 11(b) for the d -Al₆₅Co₁₅Cu₂₀ alloy, the temperature dependence of the Fermi edge follows exactly that of a Fermi-Dirac function. It is thus concluded that, similarly to i alloys, the d alloys are metals.

C. Pseudogap in DOS around E_F

As mentioned in Sec. I, almost all electronic structure calculations predict the existence of a pseudogap in the DOS around E_F . Two relevant examples are given below. The total DOS of a hypothetical 1/1 cubic approximant Al₈₀Cu₃₂Fe₁₆ to the i -Al-Cu-Fe phase, which was kindly provided by Fujiwara,⁵⁸ is shown in Fig. 12. One can notice the presence of a pseudogap with the width of about 0.5 eV and whose center is located at $E_B \approx 0.3$ eV. Figure 13 presents the total DOS of a hypothetical approximant Al₆₀Co₁₄Cu₃₀ to the d -Al-Co-Cu phase, which was kindly provided by Fujiwara.⁶⁰ A well-developed pseudogap centered approximately at E_F and of the width of about 1.0 eV is clearly visible.

In order to verify convincingly the hypothesis of a pseudogap around E_F with an experimental technique which probes the occupied electronic states directly, it is essential

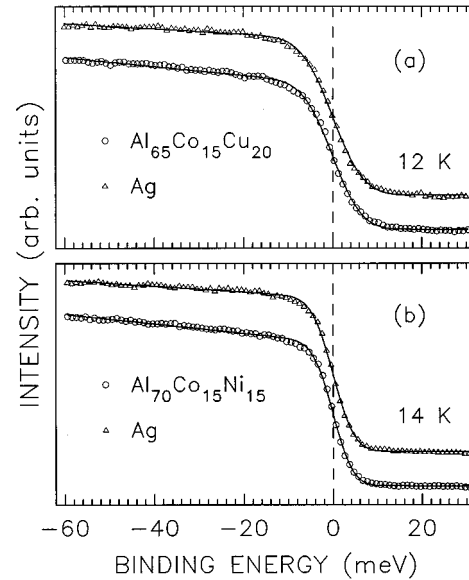


FIG. 10. Near- E_F low-temperature He I valence bands of (a) d -Al₆₅Co₁₅Cu₂₀ and Ag evaporated onto it and (b) d -Al₇₀Co₁₅Ni₁₅ and Ag evaporated onto it. The solid curves are the fits to a linearly decreasing intensity multiplied by the Fermi-Dirac function at an appropriate temperature and convoluted with a Gaussian whose FWHM is 11.8(2) in (a) and 7.0(2) meV in (b).

to distinguish between the decrease of the spectral intensity toward E_F , which results from the presence of the pseudogap, and the Fermi-edge cutoff. Such a distinction could not be achieved with previous low-energy resolution (233–500 meV), room-temperature PES studies.^{49–52,77,87,89} The spectral intensity decrease toward E_F is clearly sepa-

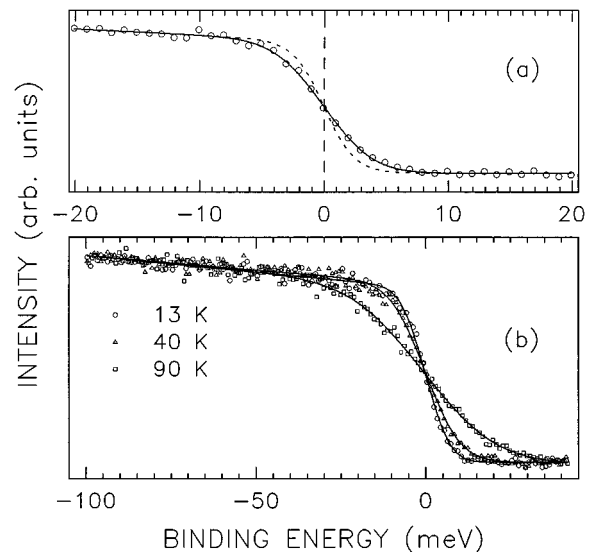


FIG. 11. (a) Near- E_F He I valence band of d -Al₆₅Co₁₅Cu₂₀ at 13 K. The solid line is a fit to a linearly decreasing intensity multiplied by the Fermi-Dirac function at 13 K (broken curve) and convoluted with a Gaussian whose FWHM is equal to 5.7(3) meV. Note that the step between the data points is 1 meV. (b) Near- E_F He I valence bands of d -Al₆₅Co₁₅Cu₂₀ measured at different temperatures. The solid lines are the fits as described in (a). Note the different E_B scales in (a) and (b).

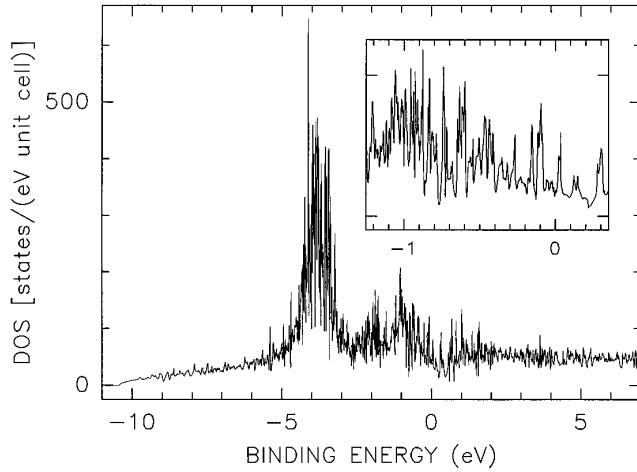


FIG. 12. Total DOS for the 1/1 *i* approximant $\text{Al}_{80}\text{Cu}_{32}\text{Fe}_{16}$ from Ref. 58. The inset shows a part of the DOS around E_F . The energy mesh used to calculate the DOS in the figure and in the inset was 0.001 and 0.0001 Ry (Ref. 58), respectively. The two ticks on the ordinate axis of the inset correspond, respectively, to 0 and 200 states/(eV unit cell).

rated from the Fermi-edge cutoff in the present high-energy resolution, low-temperature UPS spectra (Figs. 1–11).

With the aim of obtaining simple parameters to characterize the pseudogap, one can simulate the observed structure close to E_F in the valence bands of the studied QC's (Figs. 1–3 and 5) using the model proposed by Mori *et al.* (Ref. 77). As conventional alloys of the quasicrystal-forming elements do not display a DOS minimum close to E_F , it is assumed that a simple linear extrapolation of the spectra for E_B range directly before the peak of the valence band feature close to E_F accounts for the DOS without the pseudogap (the normal DOS). The presence of the pseudogap would result in an intensity dip which is assumed to be of Lorentzian shape centered at E_F , characterized by the half-width Γ_L , and the

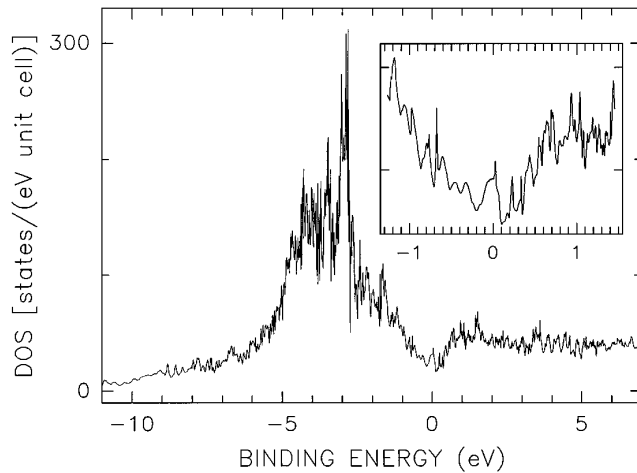


FIG. 13. Total DOS for the *d*-approximant $\text{Al}_{60}\text{Co}_{14}\text{Cu}_{30}$ from Ref. 60. The inset shows a part of the DOS around E_F . The energy meshes used to calculate the DOS in the figure and in the inset were 0.001 and 0.000 03 Ry (Ref. 60), respectively. The two ticks on the ordinate axis of the inset correspond, respectively, to 35 and 70 states/(eV unit cell).

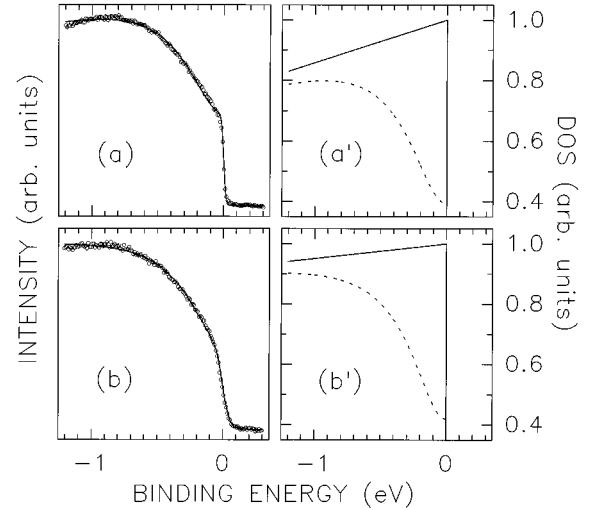


FIG. 14. He II valence-band regions (open circles) of *i*- $\text{Al}_{65}\text{Cu}_{20}\text{Fe}_{15}$ measured at (a) 14 K and (b) 283 K with the energy resolution of 31.6 (1.8) meV fitted (solid line) with Eq. (1) to the corresponding model DOS's in (a') and (b'). The solid lines in (a') and (b') represent the normal DOS at 0 K, and the broken lines show the Lorentzian dip which must be subtracted from the normal DOS in order to fit the valence-band regions in (a) and (b).

dip depth relative to the normal DOS, C . Thus the observed intensity $I(E_B)$ is the convolution of the normal DOS multiplied by the pseudogap Lorentzian function and by the Fermi-Dirac function $f(E_B, T)$, and the experimental resolution Gaussian function

$$I(E_B) = \int N(ax+b) \left(1 - \frac{C\Gamma_L^2}{x^2 + \Gamma_L^2} \right) f(x, T) \times \exp \left[-\frac{(x-E_B)^2}{2s^2} \right] dx, \quad (1)$$

where N is a normalization factor, the experimental Gaussian FWHM is related to s through a FWHM of $2\sqrt{2 \ln 2}s$, and the constants a and b are determined from a linear fit of the spectra for E_B range directly before the peak of the valence-band feature close to E_F . The C values of 0 and 100% correspond, respectively, to the normal DOS (no pseudogap) and no DOS(E_F).

1. Icosahedral alloys

We first apply the dip model described above to the valence-band regions of *i*- $\text{Al}_{65}\text{Cu}_{20}\text{Fe}_{15}$ measured at 14 and 283 K for the E_B range encompassing the feature predominantly due to Fe 3*d*-like states [Figs. 14(a) and 14(b)]. Note that for the temperature of 283 K [Fig. 14(a)], even with the high-energy resolution of 31.6(1.8) meV, the Fermi edge is hardly distinguishable from the spectral intensity decrease toward E_F . One obtains good fits of the valence-band regions close to E_F at 14 and 283 K [Figs. 14(a) and 14(b)] for values of C and Γ_L equal to 60.5(3)%, 0.36(2) eV and 58.0(6)%, 0.33(1) eV, respectively. Although the dip model used is purely phenomenological, the values arrived at for the width of the pseudogap are in good agreement with the order of magnitude expected from calculations (Fig. 12).⁵⁸

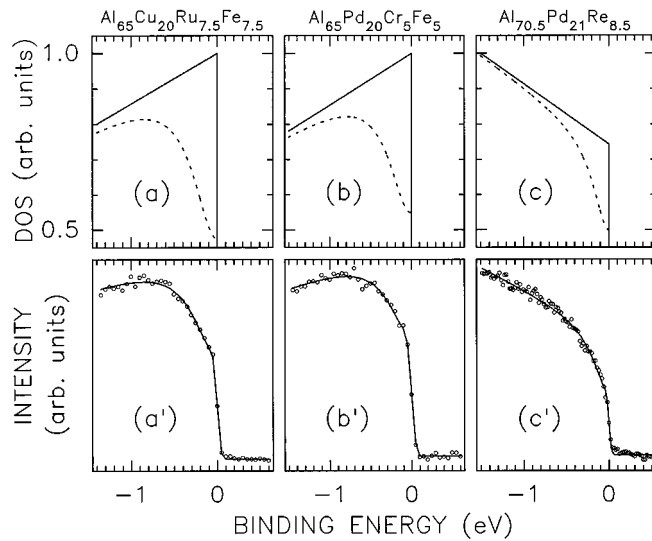


FIG. 15. The model of the DOS at 0 K which is used to fit the region of the valence band close to E_F for (a) $i\text{-Al}_{65}\text{Cu}_{20}\text{Ru}_{7.5}\text{Fe}_{7.5}$, (b) $i\text{-Al}_{70}\text{Pd}_{20}\text{Cr}_5\text{Fe}_5$, and (c) $i\text{-Al}_{70.5}\text{Pd}_{21}\text{Re}_{8.5}$. The solid lines represent the normal DOS at 0 K, whereas the broken lines represent the Lorentzian dip which must be subtracted from the normal DOS in order to fit [solid lines in (a'), (b'), and (c')], with Eq. (1), the corresponding regions of the valence bands close to E_F [open circles in (a'), (b'), and (c') are the experimental points from Figs. 2 ($i\text{-Al}_{65}\text{Cu}_{20}\text{Ru}_{7.5}\text{Fe}_{7.5}$), and 3 ($i\text{-Al}_{70}\text{Pd}_{20}\text{Cr}_5\text{Fe}_5$ and $i\text{-Al}_{70.5}\text{Pd}_{21}\text{Re}_{8.5}$), respectively].

The application of the dip model to account for the shape of the valence-band regions close to E_F for $i\text{-Al}_{65}\text{Cu}_{20}\text{Ru}_{7.5}\text{Fe}_{7.5}$, $i\text{-Al}_{70}\text{Pd}_{20}\text{Cr}_5\text{Fe}_5$, and $i\text{-Al}_{70.5}\text{Pd}_{21}\text{Re}_{8.5}$ is presented in Fig. 15. The model fits well the experimental data close to E_F . The values of C and Γ_L obtained from the fits, together with the E_B range for which the data were fitted to a line $aE_B + b$ representing the normal DOS in order to determine a and b , are given in Table I. Although there is some arbitrariness in selecting this E_B range (which leads to different values of a and b), it does not change the values of C and Γ_L significantly.

Based on the fits in Figs. 14 and 15, and on the parameters in Table I, two observations can be made. First, the two available electronic structure calculations for the approximants of the $i\text{-Al-Cu-Fe}$ (Ref. 58) and $i\text{-Al-Pd-Mn}$ (Ref. 59) phases relevant to the present study predict values

of Γ_L of a few tenths of an eV. This agrees with the values determined for $i\text{-Al}_{65}\text{Cu}_{20}\text{Fe}_{15}$, $i\text{-Al}_{64}\text{Cu}_{24}\text{Fe}_{12}$, and $i\text{-Al}_{70}\text{Pd}_{20}\text{Mn}_{10}$ alloys (Table I). Second, one would expect to observe a correlation between C , which is a measure of $1/\text{DOS}(E_F)$, and σ , assuming that the Hume-Rothery type mechanism is the main reason for the observed low values of σ in i alloys. Such a correlation is not observed (Table I). Similar values of C are found for i alloys (for example, Al-Cu-Fe and Al-Pd-Re alloys, Table I) whose values of σ differ by several orders of magnitude. This supports the idea discussed in Sec. I that the Hume-Rothery mechanism cannot be the major cause of the low values of σ .

The dip model described by Eq. (1) has a limitation, as it cannot be applied to cases where the spectral intensity is changing linearly over the wide E_B range (a few eV) below E_F . Such cases correspond to the valence bands of $i\text{-Al}_{65}\text{Cu}_{20}\text{Os}_{15}$ (Fig. 1), $i\text{-Al}_{65}\text{Cu}_{20}\text{Ru}_{15}$ and crystalline $\text{Al}_7\text{Cu}_2\text{Ru}$ (Fig. 2), and $i\text{-Zn}_{60}\text{Mg}_{32}\text{Y}_8$ (Fig. 4). One can only postulate that a pseudogap must be very wide ($\Gamma_L \geq 2$ eV) in these alloys.

It can be concluded that the simple model expressed by Eq. (1) accounts well for the shapes of valence bands close to E_F of many i alloys, and provides values for the width of a pseudogap in agreement with those predicted by the electronic structure calculations. This can thus be regarded as direct experimental evidence of the existence of a pseudogap in stable i alloys. High-resolution IPES experiments would be desirable to provide additional experimental data which, when combined with the present UPS results, would unequivocally determine the total width and depth of the pseudogap around E_F in i alloys.

An apparent observation of a shift away from E_F of the leading edge of the Al $3p$ spectra of almost all studied i alloys obtained with the Al $K\beta$ SXE technique has been claimed to represent an experimental proof for an opening of a pseudogap in these alloys.^{48,76,91} A comparison of the Al $3p$ spectra of the i phase from two such studies,^{28,91} both of which cite the uncertainty in determining the position of E_F (determined from separate XPS measurements) as 0.2 eV, is shown in Fig. 16. Whereas there is good agreement between the spectra of an Al metal [Fig. 16(a)], the leading edges of the spectra of the i alloys are shifted with respect to each other by about 1.0 eV [Fig. 16(b)], which is far beyond the claimed uncertainty of 0.2 eV in determining the position of E_F . Significant discrepancies in locating the position of

TABLE I. Pseudogap parameters from the fits with Eq. (1) of the regions of the valence bands close to E_F , as described in the text. The parameters for $i\text{-Al}_{70}\text{Pd}_{20}\text{Mn}_{10}$ are from Ref. 95.

Alloy	T (K)	E_B range for linear extrapolation (eV)	C (%)	Γ_L (eV)
$i\text{-Al}_{65}\text{Cu}_{20}\text{Fe}_{15}$	14	-1.2--0.9	60.5(3)	0.36(2)
$i\text{-Al}_{65}\text{Cu}_{20}\text{Fe}_{15}$	283	-1.2--0.9	58.0(6)	0.33(1)
$i\text{-Al}_{64}\text{Cu}_{24}\text{Fe}_{12}$	20	-1.2--0.7	55.5(6)	0.32(1)
$i\text{-Al}_{65}\text{Cu}_{20}\text{Ru}_{7.5}\text{Fe}_{7.5}$	15	-1.4--0.9	52.4(9)	0.35(1)
$i\text{-Al}_{70}\text{Pd}_{20}\text{Mn}_{10}$	15	-1.2--0.7	28.1(1.0)	0.22(2)
$i\text{-Al}_{70}\text{Pd}_{20}\text{Cr}_5\text{Fe}_5$	14	-1.5--1.0	45.1(1.1)	0.34(2)
$i\text{-Al}_{70.5}\text{Pd}_{21}\text{Re}_{8.5}$	45	-1.2--0.7	50.1(1.6)	0.21(1)
$d\text{-Al}_{65}\text{Co}_{15}\text{Cu}_{20}$	14	-2.0--1.5	80.1(4)	0.92(2)
$d\text{-Al}_{70}\text{Co}_{15}\text{Ni}_{15}$	15	-2.2--1.8	84.9(1)	1.12(1)

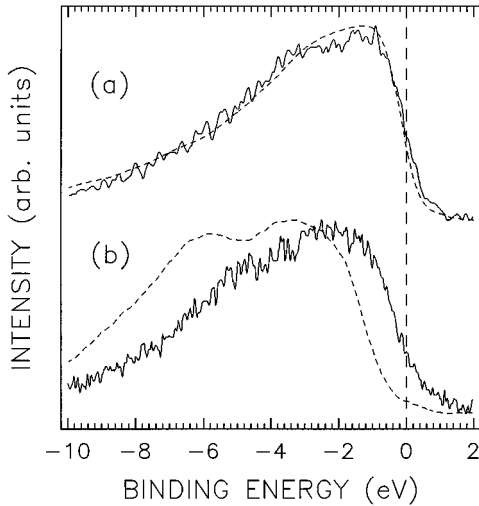


FIG. 16. A comparison of the SXE Al 3p spectra for (a) an Al metal and (b) the *i* phase from Refs. 93 (broken line) and 94 (solid line). The compositions of the *i* phase are *i*-Al_{70.5}Pd₂₁Re_{8.5} (broken line) and *i*-Al₇₀Pd₂Re₁₀ (solid line).

E_F were also noticed by comparing the SXA spectra with those calculated for the *i*-Al-Pd-Mn phase.⁵⁹ One therefore has to be cautious in interpreting the shifts of a few tenths of an eV of the leading edges associated with various orbitals from the SXE and SXA spectra.

2. Decagonal alloys

In order to apply the dip model described by Eq. (1) to the *d*-Al₆₅Co₁₅Cu₂₀ and *d*-Al₇₀Co₁₅Ni₁₅ alloys, their valence bands were measured in a narrower E_B range which encompasses only the features due to TM 3d states [Figs. 17(a) and 17(a')]. The near- E_F regions of these valence bands can be well fitted [Figs. 17(c) and 17(c')] with the dip model [Figs. 17(b) and 17(b')]. The parameters obtained from the fits are listed in Table I. The value of Γ_L obtained for *d*-Al₆₅Co₁₅Cu₂₀ agrees well with that predicted by the electronic structure calculations for the approximant of the *d* phase (Ref. 60 and Fig. 13). The dip model could not fit the near- E_F region of the valence band of the Heusler alloy Ni₂MnAl (Fig. 5). This is consistent with the fact that there is no pseudogap in this metallic alloy.

A comparison of the C and Γ_L parameters for the *i* and *d* alloys (Table I) shows that they are significantly larger for the latter than for the former. In other words, the pseudogap is deeper and wider in *d* than in *i* alloys. This is in a good agreement with the predictions of the electronic structure calculations (Figs. 12 and 13). This finding can be also taken as further evidence of the Hume-Rothery mechanism not being the major reason for the observed high values of ρ in QC's because the ρ values in *d* alloys are significantly smaller than those in *i* alloys (the larger C values for the *d* alloys than for the *i* alloys imply that the opposite should be true if the Hume-Rothery mechanism were the dominant one).

The analysis presented above leads to the conclusion that, in agreement with theoretical predictions, the observed intensity depression close to E_F in the valence bands of the stable QC's can be accounted for by the existence of the Hume-Rothery pseudogap in the DOS around E_F . This pseudogap

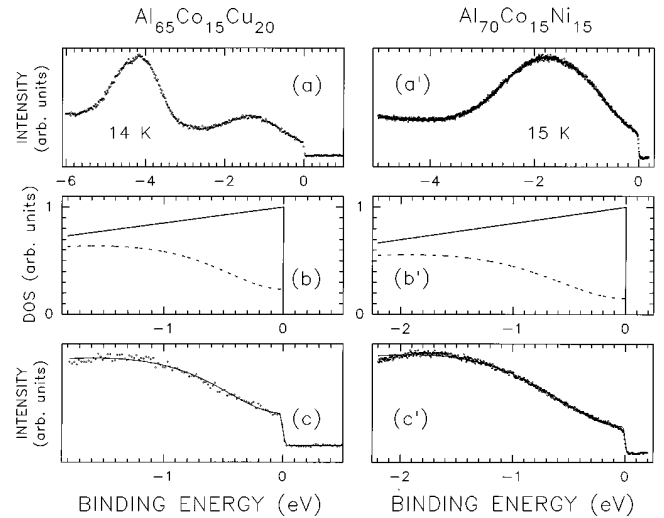


FIG. 17. Low-temperature He II valence bands of *d*-Al₆₅Co₁₅Cu₂₀ (a) and *d*-Al₇₀Co₁₅Ni₁₅ (a') measured with energy resolutions of 31.8(2.2) and 26.5(1.7) meV, respectively. The models of the DOS at 0 K [(b) and (b')] are used, respectively, to fit the near- E_F regions of the valence bands from (a) and (a'). The solid lines in (b) and (b') represent a normal DOS. The broken lines represent the dip which must be subtracted from the normal DOS in order to fit the near- E_F region of the valence bands. The near- E_F regions [(c) and (c')] of the valence bands from (a) and (a') fitted (solid line) to the models of the DOS's shown in (b) and (b') which are multiplied by the Fermi-Dirac function at 14 and 15 K, and convoluted with the respective experimental resolution Gaussian functions.

is thus an important factor which determines the stability of QC's. However, it is not the major source of the observed high- ρ values in QC's.

D. Fine structure of DOS

As discussed in Sec. I, a property specific to a quasicrystalline state seems to be the predicted fine structure (spikiness) of the DOS (Figs. 12 and 13). In order to check whether the predicted DOS spikiness can be detected with the low-temperature, high-energy-resolution UPS technique used in the present study, the theoretical valence bands in Figs. 12 and 13 have to be modified to account for the lifetime broadening effects inherent to the UPS technique,^{49,52,89} the finite resolution of an experiment, and the sample temperature. The lifetime broadening effects are represented by the Lorentzian whose FWHM is in the form $\Gamma_L^0 E_B^2$, where the Γ_L^0 parameter fixes the scale of the broadening.^{49,52,89} Figure 18 shows the occupied part of the DOS for the approximant to the *i* phase from Fig. 12 multiplied by the Fermi-Dirac function at 14 K, then convoluted with a Lorentzian to account for the lifetime broadening effects, and with a Gaussian to account for the experimental resolution. The Γ_L^0 parameter was chosen to be equal to 0.02 eV⁻¹, which is a typical value used for metallic systems.^{49,89} The chosen temperature of 14 K and the Gaussian FWHM of 31.6 meV correspond to the parameters of the experimental spectrum of *i*-Al₆₅Co₁₅Cu₂₀Fe₁₅ in Fig. 14(a). The occupied part of the DOS for the approximant to the *d* phase from Fig. 13, which was multiplied by the Fermi-Dirac function at 14 K

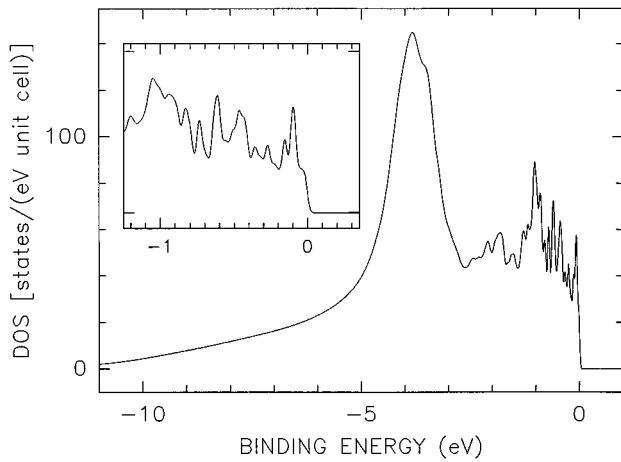


FIG. 18. Occupied part of the DOS from Fig. 12 multiplied by the Fermi-Dirac function and convoluted with a Lorentzian, to account for the lifetime broadening effects, and with a Gaussian, to account for the experimental resolution as described in the text. The value of Γ_L^0 is 0.02 eV^{-1} , whereas the temperature of 14 K and the Gaussian FWHM of 31.6 meV correspond to the experimental spectrum in Fig. 14(a). The two ticks on the ordinate axis of the inset correspond, respectively, to 0 and 100 states/(eV unit cell).

and then convoluted with a Lorentzian with $\Gamma_L^0=0.02 \text{ eV}^{-1}$ and with a Gaussian with a FWHM equal to 31.8 meV, is shown in Fig. 19. The values of the temperature and the Gaussian FWHM correspond to the experimental spectrum in Fig. 17(a).

It is clear from Figs. 18 and 19 that the predicted DOS spikiness should be observed for E_B 's up to a few eV below E_F in the experimental valence bands of both the *i* and *d* alloys measured with the high resolution of a few tens of meV. Obviously, they should be observed even more readily for the ultrahigh-energy resolution ($<10 \text{ meV}$). An inspec-

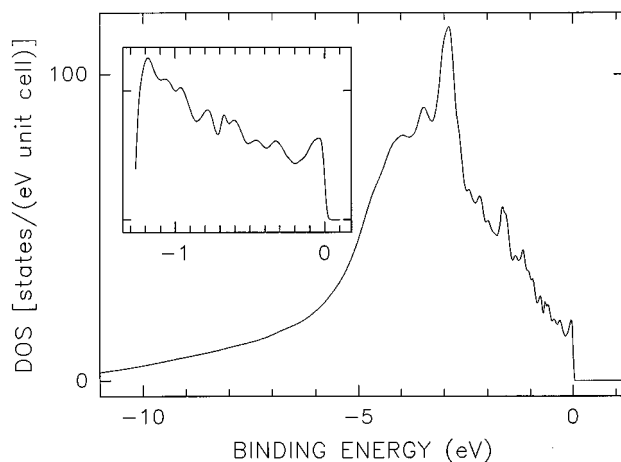


FIG. 19. Occupied part of the DOS from Fig. 13 multiplied by the Fermi-Dirac function and convoluted with a Lorentzian, to account for the lifetime broadening effects, and with a Gaussian, to account for the experimental resolution, as described in the text. The value of Γ_L^0 is 0.02 eV^{-1} , whereas the temperature of 14 K and the Gaussian FWHM of 31.8 meV correspond to the experimental spectrum in Fig. 17(a). The two ticks on the ordinate axis of the inset correspond, respectively, to 0 and 30 states/(eV unit cell).

tion of the valence bands measured with high- (Figs. 1–5, 14, and 17) and ultrahigh- (Figs. 6–11) energy resolution shows the lack of any fine structure. It must be then concluded that the predicted spikiness is not observed in the UPS spectra measured with the highest-energy resolution presently attainable.

The predicted DOS spikiness was also not observed in the recent high-energy-resolution PES study⁷⁸ of the *i*-Al₇₀Pd_{21.5}Mn_{8.5} alloy. No DOS spikiness could be detected in a NMR pressure study of the *i*-Al₆₅Cu₂₀Ru₁₅ alloy.⁹⁹ Using the tunneling spectroscopy technique, which may have an energy resolution better than perhaps 0.1 meV, Klein *et al.*¹⁰⁰ could not observe any DOS spikiness for the *i*-Al-Cu-Fe film samples.

Assuming that the predicted spikiness is not an artifact of the electronic structure calculations, the failure to detect it experimentally suggests the presence of some disorder (randomness) even in the structurally “perfect” (phason free) QC’s. Such disorder is expected¹⁰¹ to smear out the fine structure of DOS. There are some experimental facts which support this suggestion. First, local probes, such as Mössbauer spectroscopy,²³ NMR,¹⁰² and nuclear quadrupole resonance,^{102,103} clearly show the presence of distributions of the hyperfine parameters in the structurally perfect QC’s. Such distributions can only occur if there is chemical and/or topological disorder in the samples. Second, diffuse scattering is often observed in x-ray-, electron-, and neutron-diffraction patterns of high-quality, both polyquasicrystalline and single-grain QC’s.^{104,105} Its presence indicates that some disorder must be present in the diffracting structure. Third, a recent study¹⁰⁶ on the propagation of acoustic shear waves in a single-grain *i*-Al-Pd-Mn shows similarities between the acoustic properties of this alloy and those of amorphous metals. Fourth, the success of quantum interference theories,^{2–4,8} which were originally developed for disordered conductors, in accounting for the temperature and field dependencies of the electrical conductivity and magnetoresistance of several stable *i* alloys indicates that these alloys are electronically disordered.¹⁰⁷ From a structural point of view, QC’s could be considered intrinsically random if they are stabilized by entropy,¹⁰⁸ and thus if their structure could be described by a random tiling model. A recent random tiling model¹⁰⁹ for the *i*-Al-Cu-Fe and *i*-Al-Pd-Mn phases indicates that partial chemical disorder is an inevitable part of the quasicrystalline structure. Thus the presence of disorder, which may be an intrinsic feature of the quasiperiodic systems, would wash out the predicted spikiness in the DOS, and could explain why this spikiness cannot be detected experimentally.

E. Quasiperiodicity and unusual physical properties

The main effort in the physics of QC’s has been to establish whether quasiperiodicity leads to physical properties which are distinct from those in the crystalline and/or amorphous alloys of similar compositions. The electronic structure results presented here show no unusual features that could be the consequence of the quasiperiodic order. Although the pseudogap around E_F seems to be a generic property of QC’s, it is also present in both the amorphous⁷³ and crystalline^{74,75} systems. The predicted DOS spikiness, which could be a distinct feature associated only with QC’s, could

not be detected in the PES spectra measured with the highest-energy resolution presently available. One also observes close similarity between the PES and SXE spectra of QC's and crystalline alloys of similar compositions (Fig. 2 and Refs. 48, 87, 89, and 110).

Perhaps the most dramatic realization that quasiperiodicity is not essential for the observation of unusual physical properties came with the observation that such properties can also occur in the approximants of QC's. For example, low values of σ , and its increase with temperature were found in the approximants to the *i*-Mg-Ga-Al-Zn, *i*-Al-Cu-Fe, and *i*-Al-Mn(Si) phases^{8,15,16,68,111,112} and in several *d* approximants along the pseudoquasiperiodic planes.¹¹³ Similarities were also observed between the values and/or temperature and/or magnetic field dependencies of the Hall coefficient,^{15,112} thermoelectric power,¹⁵ magnetoresistance,¹¹² optical conductivity,³³ γ ,^{15,112,114} and local hyperfine parameters^{23,46,115} in the *i* alloys and their approximants.

The experimental results described above lead to the conclusion that it is the complex local atomic order rather than long-range quasiperiodic order which determines the unusual properties of alloys. In retrospect, this is perhaps not surprising since there is no physical basis to expect that classically forbidden symmetries occurring in QC's should lead to physical properties distinctly different from those in crystalline systems.

IV. SUMMARY

We have performed low-temperature UPS experiments with high- and ultrahigh-energy resolution on a series of stable *i* and *d* alloys. We have shown that, contrary to the claims made in the literature, all studied QC's have a clearly developed Fermi edge, and are therefore metallic down to the temperature of measurement (12–45 K). The decrease of the spectral intensity toward E_F has been shown to be compatible with the presence of the theoretically predicted pseudogap in the DOS around E_F . This gap has been found to be much wider in *d* alloys than in *i* alloys. The presence of the theoretically predicted fine structure of the DOS has not been observed even with a resolution of 5 meV. The similar values and dependencies of various physical parameters of QC's and of their approximants indicates that it is the complex local atomic order, rather than the long-range quasiperiodic order, which determines their unusual behavior. A review of the electronic properties of QC's has also been presented.

ACKNOWLEDGMENTS

This work was supported by the Natural Sciences and Engineering Research Council of Canada, the Fonds National Suisse de la Recherche Scientifique, and the Ministry of Education, Science, and Culture of Japan.

* Author to whom correspondence should be addressed.

¹D. Shechtman, I. Blech, D. Gratias, and J. W. Cahn, *Phys. Rev. Lett.* **53**, 1951 (1984).

²*Proceedings of the 5th International Conference on Quasicrystals*, edited by C. Janot and R. Mosseri (World Scientific, Singapore, 1995).

³*Aperiodic '94, Proceedings of the International Conference on Aperiodic Crystals*, edited by G. Chapuis and W. Paciorek (World Scientific, Singapore, 1995); C. Janot, *Quasicrystals: A Primer*, 2nd ed. (Oxford University Press, New York, 1994).

⁴*Quasicrystals, The State of the Art*, edited by D. P. DiVincenzo and P. J. Steinhardt (World Scientific, Singapore, 1991).

⁵*Quasicrystals*, edited by T. Fujiwara and T. Ogawa (Springer-Verlag, Berlin, 1990).

⁶N. Wang, H. Chen, and K. H. Kuo, *Phys. Rev. Lett.* **59**, 1010 (1987); J. C. Jiang, K. K. Fung, and K. H. Kuo, *ibid.* **68**, 616 (1992).

⁷T. Ishimasa, H.-U. Nissen, and Y. Fukano, *Phys. Rev. Lett.* **55**, 511 (1985); H. Chen, D. X. Li, and K. H. Kuo, *ibid.* **60**, 1645 (1988).

⁸S. Takeuchi, *Mater. Sci. Forum* **150-151**, 35 (1994), and references therein; S. J. Poon, *Adv. Phys.* **41**, 303 (1992), and references therein.

⁹C. A. Guryan, A. I. Goldman, P. W. Stephens, K. Hiraga, A. P. Tsai, A. Inoue, and T. Masumoto, *Phys. Rev. Lett.* **62**, 2409 (1989); P. A. Bancel, *ibid.* **63**, 2741 (1989); M. De Boissieu, M. Durand Charre, P. Bastie, A. Carabelli, M. Boudard, M. Besiere, S. Lefebvre, C. Janot, and M. Audier, *Philos. Mag. Lett.* **65**, 147 (1992).

¹⁰S. W. Kycia, A. I. Goldman, T. A. Lograsso, D. W. Delaney, D. Black, M. Sutton, E. Dufresne, R. Brünig, and B. Rodricks, *Phys. Rev. B* **48**, 3544 (1993).

¹¹A. Sahnoune, J. O. Ström-Olsen, and A. Zaluska, *Phys. Rev. B* **46**, 10 629 (1992).

¹²T. Klein, C. Berger, G. Fourcaudot, J. C. Grieco, and F. Cyrot-Lackmann, *J. Non-Cryst. Solids* **156-158**, 901 (1993).

¹³R. Haberkern, G. Fritsch, and J. Schilling, *Z. Phys. B* **92**, 383 (1993).

¹⁴P. Lindqvist, C. Berger, T. Klein, P. Lanco, F. Cyrot-Lackmann, and Y. Calvayrac, *Phys. Rev. B* **48**, 630 (1993).

¹⁵F. S. Pierce, P. A. Bancel, B. D. Biggs, Q. Guo, and S. J. Poon, *Phys. Rev. B* **47**, 5670 (1993).

¹⁶D. Mayou, C. Berger, F. Cyrot-Lackmann, T. Klein, and P. Lanco, *Phys. Rev. Lett.* **70**, 3915 (1993).

¹⁷M. A. Chernikov, A. Bernasconi, C. Beeli, and H. R. Ott, *Europhys. Lett.* **21**, 767 (1993).

¹⁸H. Akiyama, T. Hashimoto, T. Shibuya, K. Edagawa, and S. Takeuchi, *J. Phys. Soc. Jpn.* **62**, 639 (1993).

¹⁹P. Lanco, T. Klein, C. Berger, F. Cyrot-Lackmann, G. Fourcaudot, and A. Sulpice, *Europhys. Lett.* **18**, 227 (1992); P. Lanco, C. Berger, F. Cyrot-Lackmann, and A. Sulpice, *J. Non-Cryst. Solids* **153-154**, 325 (1993).

²⁰C. Berger, T. Grenet, P. Lindqvist, P. Lanco, J. C. Grieco, G. Fourcaudot, and F. Cyrot-Lackmann, *Solid State Commun.* **87**, 977 (1993).

²¹B. D. Biggs, S. J. Poon, and N. R. Munirathnam, *Phys. Rev. Lett.* **65**, 2700 (1990).

²²N. P. Lala, R. S. Tiwari, and O. N. Srivastava, *J. Phys. Condens. Matter* **7**, 2409 (1995); N. P. Lalla, R. S. Tiwari, O. N. Srivastava, B. Schnell, and G. Thummes, *Z. Phys. B* **99**, 43 (1995).

²³Z. M. Stadnik, in *Mössbauer Spectroscopy Applied to Magnetism and Materials Science*, edited by G. J. Long and F. Grandjean (Plenum, New York, 1996), Vol. 2, Chap. 6, p. 125.

²⁴Y. Honda, K. Edagawa, S. Takeuchi, A.-P. Tsai, and A. Inoue, *Jpn. J. Appl. Phys. A* **34**, 2415 (1995).

- ²⁵H. Akiyama, Y. Honda, T. Hashimoto, K. Edagawa, and A. Takeuchi, *Jpn. J. Appl. Phys. B* **7**, L1003 (1993); Y. Honda, K. Edagawa, A. Yoshika, T. Hashimoto, and S. Takeuchi, *Jpn. J. Appl. Phys. A* **9**, 4929 (1994).
- ²⁶F. S. Pierce, S. J. Poon, and Q. Guo, *Science* **261**, 737 (1993).
- ²⁷F. S. Pierce, Q. Guo, and S. J. Poon, *Phys. Rev. Lett.* **73**, 2220 (1994).
- ²⁸T. Takeuchi, Y. Yamada, U. Mizutani, Y. Honda, K. Edagawa, and S. Takeuchi, in *Proceedings of the 5th International Conference on Quasicrystals* (Ref. 2), p. 534.
- ²⁹C. Gignoux, C. Berger, G. Fourcaudot, J. C. Grieco, and F. Cyrot-Lackmann, in *Proceedings of the 5th International Conference on Quasicrystals* (Ref. 2), p. 452.
- ³⁰N. Mott, *Conduction in Non-Crystalline Materials* (Clarendon, Oxford, 1993).
- ³¹R. Tamura, A. Waseda, K. Kimura, and H. Ino, *Phys. Rev. B* **50**, 9640 (1994).
- ³²C. C. Homes, T. Timusk, X. Wu, Z. Altounian, A. Sahnoune, and J. O. Ström-Olsen, *Phys. Rev. Lett.* **67**, 2694 (1991).
- ³³X. Wu, C. C. Homes, S. E. Burkov, T. Timusk, F. S. Pierce, S. J. Poon, S. L. Cooper, and M. A. Karlow, *J. Phys. Condens. Matter* **5**, 5975 (1993).
- ³⁴M. A. Chernikov, A. Bianchi, and H. R. Ott, *Phys. Rev. B* **51**, 153 (1995).
- ³⁵M. A. Chernikov, A. Bianchi, E. Felder, U. Gubler, and H. R. Ott, *Europhys. Lett.* **35**, 431 (1996).
- ³⁶S. Matsuo, T. Ishimasa, H. Nakano, and Y. Fukano, *J. Phys. F* **18**, L175 (1988); Z. M. Stadnik, G. Stroink, H. Ma, and G. Williams, *Phys. Rev. B* **39**, 9797 (1989); T. Klein, C. Berger, D. Mayou, and F. Cyrot-Lackmann, *Phys. Rev. Lett.* **66**, 2907 (1991).
- ³⁷L. Shu-yuan, W. Xue-mei, L. Li, Z. Dian-lin, L. X. He, and K. X. Kuo, *Phys. Rev. B* **41**, 9625 (1990); T. Shibuya, T. Hashimoto, and S. Takeuchi, *J. Phys. Soc. Jpn.* **59**, 1917 (1990); S. Martin, A. F. Hebard, A. R. Kortan, and F. A. Thiel, *Phys. Rev. Lett.* **67**, 719 (1991); W. Yun-ping and Z. Dian-lin, *Phys. Rev. B* **49**, 13 204 (1994).
- ³⁸Z. Dian-lin, L. Li, W. Xue-mei, L. Shu-yuan, L. X. He, and K. H. Kuo, *Phys. Rev. B* **41**, 8557 (1990); Z. Dian-lin, C. Shao-chun, W. Yun-ping, L. Li, W. Xue-mei, X. L. Ma, and K. H. Kuo, *Phys. Rev. Lett.* **66**, 2778 (1991); W. Yun-ping, Z. Dian-lin, and L. F. Chen, *Phys. Rev. B* **48**, 10 542 (1993).
- ³⁹D.N. Basov, T. Timusk, F. Barakat, J. Greedan, and B. Grushko, *Phys. Rev. Lett.* **72**, 1937 (1994).
- ⁴⁰R. Lück and S. Kek, *J. Non-Cryst. Solids* **153-154**, 329 (1993).
- ⁴¹W. Hume-Rothery, *J. Inst. Metals* **35**, 295 (1926); *The Metallic State* (Oxford University Press, London, 1931).
- ⁴²H. Jones, *Proc. Phys. Soc.* **49**, 250 (1937); N. F. Mott and H. Jones, *The Theory of the Properties of Metals and Alloys* (Oxford University Press, Glasgow, 1958).
- ⁴³P. A. Bancel and P. A. Heiney, *Phys. Rev. B* **33**, 7917 (1986); A.-P. Tsai, A. Inoue, and T. Masumoto, *Mater. Trans., Jpn. Inst. Met.* **30**, 464 (1989); **30**, 666 (1989); A. Inoue, A.-P. Tsai, and T. Masumoto, in *Quasicrystals* (Ref. 5), p. 80.
- ⁴⁴J. Friedel and F. Dénoyer, *C.R. Acad. Sci. Paris* **305**, 171 (1987); A. P. Smith and N. W. Ashcroft, *Phys. Rev. Lett.* **59**, 1365 (1987); V. G. Vaks, V. V. Kamysenko, and G. D. Samolyuk, *Phys. Lett. A* **132**, 131 (1988); J. Friedel, *Helv. Phys. Acta* **61**, 538 (1988); *Philos. Mag. B* **65**, 1125 (1992).
- ⁴⁵K. Kimura, H. Iwahashi, T. Hashimoto, S. Takeuchi, U. Mizutani, S. Ohashi, and G. Itoh, *J. Phys. Soc. Jpn.* **58**, 2472 (1989); J. L. Wagner, B. D. Biggs, and S. J. Poon, *Phys. Rev. Lett.* **65**, 203 (1990).
- ⁴⁶F. Hippert, L. Kandel, Y. Calvayrac, and B. Dubost, *Phys. Rev. Lett.* **69**, 2086 (1992); E. A. Hill, T. C. Chang, Y. Wu, S. J. Poon, F. S. Pierce, and Z. M. Stadnik, *Phys. Rev. B* **49**, 8615 (1994).
- ⁴⁷S. E. Burkov, T. Timusk, and N. W. Ashcroft, *J. Phys. Condens. Matter* **4**, 9447 (1992); L. Degiorgi, M. A. Chernikov, C. Beeli, and H. R. Ott, *Solid State Commun.* **87**, 721 (1993); D. Macko and M. Kašpárková, *Philos. Mag. Lett.* **67**, 307 (1993).
- ⁴⁸E. Belin, Z. Dankhazi, and A. Sadoc, *Mater. Sci. Eng. A* **181-182**, 717 (1994), and references therein; U. Mizutani, Y. Yamada, T. Takeuchi, K. Hashimoto, E. Belin, A. Sadoc, T. Yamauchi, and T. Matsuda, *J. Phys. Condens. Matter* **6**, 7335 (1994); E. Belin, Z. Dankházi, A. Sadoc, and J. M. Dubois, *ibid.* **6**, 8771 (1994), and references therein.
- ⁴⁹G. W. Zhang, Z. M. Stadnik, A.-P. Tsai, A. Inoue, and T. Miyazaki, *Z. Phys. B* **97**, 439 (1995), and references therein; Z. M. Stadnik, G. W. Zhang, A.-P. Tsai, and A. Inoue, *Phys. Rev. B* **51**, 4023 (1995), and references therein.
- ⁵⁰H. Matsubara, S. Ogawa, T. Kinoshita, K. Kishi, S. Takeuchi, K. Kimura, and S. Suga, *Jpn. J. Appl. Phys. A* **30**, L389 (1991).
- ⁵¹L. E. Depero and F. Parmigiani, *Chem. Phys. Lett.* **214**, 208 (1993).
- ⁵²Z. M. Stadnik, G. W. Zhang, A.-P. Tsai, and A. Inoue, *Phys. Rev. B* **51**, 11 358 (1995); *Phys. Lett. A* **198**, 237 (1995).
- ⁵³M. A. Fradkin, *J. Phys. Condens. Matter* **4**, 10497 (1992); A. E. Carlsson, *Phys. Rev. B* **47**, 2515 (1993).
- ⁵⁴T. Fujiwara and T. Yokokawa, *Phys. Rev. Lett.* **66**, 333 (1991).
- ⁵⁵J. Hafner and M. Krajčí, *Phys. Rev. B* **47**, 11 795 (1993); *Phys. Rev. Lett.* **68**, 2321 (1992).
- ⁵⁶T. Fujiwara, S. Yamamoto, and G. Trambly de Laissardière, *Phys. Rev. Lett.* **71**, 4166 (1993).
- ⁵⁷M. Windisch, M. Krajčí, and J. Hafner, *J. Phys. Condens. Matter* **6**, 6977 (1994), and references therein.
- ⁵⁸G. Trambly de Laissardière and T. Fujiwara, *Phys. Rev. B* **50**, 5999 (1994), and references therein.
- ⁵⁹M. Krajčí, M. Windisch, J. Hafner, G. Kresse, and M. Mihalkovič, *Phys. Rev. B* **51**, 17 355 (1995), and references therein.
- ⁶⁰G. Trambly de Laissardière and T. Fujiwara, *Phys. Rev. B* **50**, 9843 (1994).
- ⁶¹S. E. Burkov, *Phys. Rev. Lett.* **67**, 614 (1991); *J. Phys. (France) I* **2**, 695 (1992); *Phys. Rev. B* **47**, 12 325 (1993).
- ⁶²R. F. Sabiryanov and S. K. Bose, *J. Phys. Condens. Matter* **6**, 6197 (1994); **7**, 2375E (1995); R. F. Sabiryanov, S. K. Bose, and S. E. Burkov, *ibid.* **7**, 5437 (1995).
- ⁶³K. Wang, C. Scheidt, P. Garoche, and Y. Calvayrac, *J. Phys. (France) I* **2**, 1553 (1992).
- ⁶⁴S. E. Burkov, A. A. Varlamov, and D. V. Livanov, *Phys. Rev. B* **53**, 11 504 (1996).
- ⁶⁵J. C. Phillips and K. M. Rabe, *Phys. Rev. Lett.* **66**, 923 (1991).
- ⁶⁶J. C. Phillips, *Solid State Commun.* **83**, 379 (1992); *Phys. Rev. B* **47**, 2522 (1993); **47**, 7747 (1993).
- ⁶⁷T. Klein and O. G. Symko, *Phys. Rev. Lett.* **73**, 2248 (1994).
- ⁶⁸C. Berger, D. Mayou, and F. Cyrot-Lackmann, in *Proceedings of the 5th International Conference on Quasicrystals* (Ref. 2), p. 423.
- ⁶⁹K. Kimura and S. Takeuchi, in *Quasicrystals, The State of the Art* (Ref. 4), p. 313; K. Kimura, K. Kishi, T. Hashimoto, and S. Takeuchi, in *Quasicrystals*, edited by K. H. Kuo and T. Nishimiyama (World Scientific, Singapore, 1991).

- ⁷⁰C. Janot, Phys. Rev. B **53**, 181 (1996).
- ⁷¹C. Janot and M. de Boissieu, Phys. Rev. Lett. **72**, 1674 (1994).
- ⁷²K. Mouloupoulos and F. Cyrot-Lackmann, in *Proceedings of the 5th International Conference on Quasicrystals* (Ref. 2), p. 596.
- ⁷³P. Häussler, in *Glassy Metals III*, edited by H. Beck and H.-J. Güntherodt (Springer-Verlag, Berlin, 1994), p. 163, and references therein.
- ⁷⁴A. E. Carlsson and P. J. Meschter, in *Intermetallic Compounds*, edited by J. H. Westbrook and R. L. Fleischer (Wiley, Chichester, 1995), Vol. I, p. 55, and references therein.
- ⁷⁵G. Trambly de Laissardière, D. Nguyen Manh, L. Magaud, J. P. Julien, F. Cyrot-Lackmann, and D. Mayou, Phys. Rev. B **52**, 7920 (1995).
- ⁷⁶E. Belin, Z. Dankhazi, A. Sadoc, J. M. Dubouis, and Y. Calvayrac, Europhys. Lett. **26**, 677 (1994).
- ⁷⁷M. Mori, S. Matsuo, T. Ishimasa, T. Matsuura, K. Kamiya, H. Inokuchi, and T. Matsukawa, J. Phys. Condens. Matter **3**, 767 (1991).
- ⁷⁸X. Wu, S. W. Kycia, C. G. Olson, P. J. Benning, A. I. Goldman, and D. W. Lynch, Phys. Rev. Lett. **75**, 4540 (1995).
- ⁷⁹M. Grioni, D. Malterre, and Y. Baer, J. Low Temp. Phys. **99**, 195 (1995).
- ⁸⁰A.-P. Tsai, A. Inoue, and T. Masumoto, Jpn. J. Appl. Phys. **26**, L1505 (1987); K. Hiraga, B.-P. Zhang, M. Hirabayashi, A. Inoue, and T. Masumoto, *ibid.* **27**, L951 (1988).
- ⁸¹A.-P. Tsai, A. Inoue, and T. Masumoto, Jpn. J. Appl. Phys. **27**, L1587 (1988).
- ⁸²A. P. Tsai, A. Inoue, Y. Yokoyama, and T. Masumoto, Mater. Trans. JIM **31**, 98 (1990); Philos. Mag. Lett. **61**, 9 (1990).
- ⁸³Y. Yokoyama, A.-P. Tsai, A. Inoue, T. Masumoto, and H. S. Chen, Mater. Trans. JIM **32**, 421 (1991); A. P. Tsai, Y. Yokoyama, A. Inoue, and T. Masumoto, in *Physics and Chemistry of Finite Systems: From Clusters to Crystals*, edited by P. Jena, S. N. Khanna, and B. K. Rao (Kluwer, Amsterdam, 1992), Vol. I, p. 177.
- ⁸⁴A. Niikura, A.-P. Tsai, A. Inoue, and T. Masumoto, Philos. Mag. Lett. **69**, 351 (1994); Jpn. J. Appl. Phys. A **33**, L1538 (1994); A.-P. Tsai, A. Niikura, A. Inoue, and T. Masumoto, in *Proceedings of the 5th International Conference on Quasicrystals* (Ref. 2), p. 628.
- ⁸⁵A.-P. Tsai, A. Inoue, and T. Masumoto, Mater. Trans. JIM **30**, 300 (1989); **30**, 463 (1989); A. R. Kortan, F. A. Thiel, H. S. Chen, A.-P. Tsai, A. Inoue, and T. Masumoto, Phys. Rev. B **40**, 9397 (1989).
- ⁸⁶B. Grushko, U. Lemmerz, and C. Freiburg, Philos. Mag. Lett. **70**, 261 (1994).
- ⁸⁷Z. M. Stadnik and G. Stroink, Phys. Rev. B **47**, 100 (1993).
- ⁸⁸J.-J. Yeh, *Atomic Calculation of Photoionization Cross-Sections and Asymmetry Parameters* (Gordon and Breach, New York, 1993).
- ⁸⁹G. W. Zhang and Z. M. Stadnik, in *Proceedings of the 5th International Conference on Quasicrystals* (Ref. 2), p. 552; G. W. Zhang, Z. M. Stadnik, A.-P. Tsai, and A. Inoue, Phys. Rev. B **50**, 6696 (1994); Phys. Lett. A **186**, 345 (1994).
- ⁹⁰U. Mizutani, Y. Yamada, T. Takeuchi, K. Hashimoto, E. Belin, A. Sadoc, T. Yamauchi, and T. Matsuda, J. Phys. Condens. Matter **6**, 7335 (1994).
- ⁹¹E. Belin, Z. Dankhazi, A. Sadoc, M. Flank, J. S. Poon, H. Müller, and H. Kirchmayr, in *Proceedings of the 5th International Conference on Quasicrystals* (Ref. 2), p. 435.
- ⁹²T. Takeuchi, Y. Yamada, U. Mizutani, Y. Honda, K. Edagawa, and S. Takeuchi, in *Proceedings of the 5th International Conference on Quasicrystals* (Ref. 2), p. 534.
- ⁹³R. T. Poole, P. C. Kemeny, J. Liesegang, J. G. Jenkin, and R. C. G. Leckey, J. Phys. F **3**, L46 (1973).
- ⁹⁴J. A. R. Samson, *Techniques of Vacuum Ultraviolet Spectroscopy* (Wiley, New York, 1967).
- ⁹⁵Z. M. Stadnik, D. Purdie, M. Garnier, Y. Baer, A.-P. Tsai, A. Inoue, K. Edagawa, and S. Takeuchi, Phys. Rev. Lett. **77**, 1777 (1996).
- ⁹⁶The temperature was determined from the width of the Fermi edge in the photoemission spectrum of Ag evaporated on the sample after it had been measured. This width was always in agreement with that displayed in spectra from the sample itself.
- ⁹⁷M. Terauchi, M. Tanaka, A.-P. Tsai, A. Inoue, and T. Masumoto, Philos. Mag. Lett. **74**, 107 (1996).
- ⁹⁸D. N. Basov, T. Timusk, F. Pierce, P. Volkov, Q. Guo, S. J. Poon, G. A. Thomas, D. Rapkine, A. R. Kortan, F. Barakat, J. Greedan, and B. Grushko, in *Proceedings of the 5th International Conference on Quasicrystals* (Ref. 2), p. 564.
- ⁹⁹A. Shastri, D. B. Baker, M. S. Conradi, F. Borsa, and D. R. Torgeson, Phys. Rev. B **52**, 12 681 (1995).
- ¹⁰⁰T. Klein, O. G. Symko, D. N. Davydov, and A. G. M. Jansen, Phys. Rev. Lett. **74**, 3656 (1995).
- ¹⁰¹S. Yamamoto and T. Fujiwara, Phys. Rev. B **51**, 8841 (1995).
- ¹⁰²A. Shastri, F. Borsa, D. R. Torgeson, J. E. Shield, and A. I. Goldman, Phys. Rev. B **50**, 15 651 (1994).
- ¹⁰³A. Shastri, F. Borsa, D. R. Torgeson, and A. I. Goldman, Phys. Rev. B **50**, 4224 (1994).
- ¹⁰⁴K. Hradil, T. Proffen, F. Frey, K. Eichhorn, and S. Kek, Philos. Mag. Lett. **71**, 199 (1995); L. E. Levine and J. L. Libbert, *ibid.* **71**, 213 (1995).
- ¹⁰⁵M. De Boissieu, M. Boudard, B. Hennion, R. Bellissent, S. Kycia, A. Goldman, C. Janot, and M. Audier, Phys. Rev. Lett. **75**, 89 (1995).
- ¹⁰⁶N. Vernier, G. Bellessa, B. Perrin, A. Zarembovitch, and M. De Boissieu, Europhys. Lett. **22**, 187 (1993).
- ¹⁰⁷M. Ahlgren, M. Rodmar, Th. Klein, and Ö. Rapp, Phys. Rev. B **51**, 7287 (1995).
- ¹⁰⁸C. L. Heinley, in *Quasicrystals and Incommensurate Structures in Condensed Matter*, edited by M. J. Yacamán, D. Romeu, V. Castaño, and A. Gómez (World Scientific, Singapore, 1990), p. 152; M. Widom, in *Quasicrystals*, edited by M. V. Jarić and S. Lindqvist (World Scientific, Singapore, 1990), p. 337; C. L. Henley, in *Quasicrystals, The State of the Art* (Ref. 4), p. 429.
- ¹⁰⁹V. Elser, Philos. Mag. B **73**, 641 (1996).
- ¹¹⁰T. Takeuchi and U. Mizutani, Phys. Rev. B **52**, 9300 (1995).
- ¹¹¹K. Edagawa, N. Naito, and S. Takeuchi, Philos. Mag. B **65**, 1011 (1992).
- ¹¹²C. Berger, C. Gignoux, O. Tjernberg, P. Lindqvist, F. Cyrot-Lackmann, and Y. Calvayrac, Physica B **204**, 44 (1995).
- ¹¹³P. Volkov and S. J. Poon, Phys. Rev. B **52**, 12 685 (1995).
- ¹¹⁴U. Mizutani, A. Kamiya, T. Matsuda, K. Kishi, and S. Takeuchi, J. Phys. Condens. Matter **3**, 3711 (1991).
- ¹¹⁵F. Hippert, R. A. Brand, J. Pelloth, and Y. Calvayrac, J. Phys. Condens. Matter **6**, 11 189 (1994).